Journal of Physics: Conference Series **569** (2014) 012027 doi:10.1088/1742-6596/569/1/012027

^{16}O + ^{16}O + valence neutrons in molecular orbitals structures of positive- and negative-parity superdeformed bands in ^{34}S

Yasutaka Taniguchi

Department of Medical and General Sciences, Nihon Institute of Medical Science, Shimogawara 1276, Moroyama-machi, Iruma-gun, Saitama 350-0435, Japan

E-mail: yasutaka@nims.ac.jp

Abstract. The structures of superdeformed (SD) states in ^{34}S are investigated using the antisymmetrized molecular dynamics and generator coordinate method (GCM). The GCM basis wave functions are calculated via energy variation with a constraint on the quadrupole deformation parameter β. By applying the GCM after parity and angular momentum projections, the coexistence of two positive- and one negative-parity SD bands are predicted, and low-lying states and other deformed bands are obtained. The SD bands have structures of ^{16}O + ^{16}O + two valence neutrons in molecular orbitals around the two ^{16}O cores in a cluster picture. The configurations of the two valence neutrons are δ^2 and π^2 for the positive-parity SD bands and $\pi^1\delta^1$ for the negative-parity SD band.

1. Introduction

Dynamic structural changes under excitation are significant properties of nuclei. Superdeformation and clustering are typical changes. Clustering is a typical structure in the light mass region. To clarify the dynamic structural changes of nuclei, it is necessary to study the nuclear structure in terms of both deformation and clustering. However, those studies have been insufficient.

S isotopes ($Z = 16$) are suitable nuclei for studying deformation and clustering caused by excitation. S isotopes are expected to be favorable for the formation of superdeformed (SD) bands because $Z = 16$ is considered a magic number of superdeformation. The existence of SD bands in S isotopes has been discussed in the frameworks of a mean-field model[1], a cluster model[2], and antisymmetrized molecular dynamics (AMD)[3]. In terms of clustering, S isotopes are key nuclei in the *sd* shell. S isotopes are analogs of Be isotopes because those isotopes can form systems consisting of two doubly closed shell nuclei (^{16}O and α for S and Be isotopes, respectively) and valence neutrons. In Be isotopes, structures consisting of α + α + valence neutrons in molecular orbitals are thought to develop in low-lying states, with the valence neutrons in molecular orbitals around two α cores[4–11]. The SD states in ^{32}S are predicted to contain a large amount of ^{16}O + ^{16}O cluster structure components[2, 3]. They suggest the existence of SD states that have ^{16}O + ^{16}O + valence neutrons in the molecular orbital structure in S isotopes.

By a γ spectroscopy experiment, the structures in ^{34}S are investigated up to the $J^\pi = 10^+$ and (9^-) states for positive- and negative-parity states, respectively, mainly for the yrast states[12].

Content from this work may be used under the terms of the Creative Commons Attribution 3.0 licence. Any further distribution of this work must maintain attribution to the author(s) and the title of the work, journal citation and DOI.
Published under licence by IOP Publishing Ltd

In contrast to the yrast states, the structures of the non-yrast states with mp-mh configurations have never been clarified.

This paper aims to clarify the structures of SD states in ^{34}S using AMD and the generator coordinate method (GCM). The coexistence of positive- and negative-parity SD bands and their structures are discussed, focusing on ^{16}O + ^{16}O + valence neutrons in molecular orbitals around the two ^{16}O cores.

2. Framework

The wave functions in low-lying states are obtained using parity projection and angular momentum projection (AMP) and the GCM with deformed-basis AMD wave functions. A deformed-basis AMD wave function $|\Phi\rangle$ is a Slater determinant of Gaussian wave packets.

The basis wave functions of the GCM are obtained by energy variation with a constraint potential $V_{\rm cnst}$ after projection onto eigenstates of parity. The Gogny D1S force is used as the effective interaction.

To obtain the deformed wave functions, the constraint potential $V_{\rm cnst}$ for the matter quadrupole deformation parameter β of the total system is used. The optimized wave functions are superposed after parity projection and AMP by employing the quadrupole deformation parameter β,

$$\left|\Phi^{J\pi}_{M}\right\rangle = \sum_{i} f_i \hat{P}^{J\pi}_{MK_i} \left|\Phi(\beta_i)\right\rangle , \tag{1}$$

where $\hat{P}^{J^\pi}_{MK}$ is the parity and total angular momentum projection operator, and $|\Phi(\beta_i)\rangle$ are optimized wave functions with a constraint for $\beta = \beta_i$. The coefficients f_i are determined by the Hill–Wheeler equation,

$$\delta\left(\left\langle \Phi^{J\pi}_{M}\right| \hat{H} \left|\Phi^{J\pi}_{M}\right\rangle - \epsilon \left\langle \Phi^{J\pi}_{M}\middle|\Phi^{J\pi}_{M}\right\rangle\right) = 0. \tag{2}$$

Then we obtain the energy spectra and the corresponding wave functions, which are expressed by the superposition of the optimum wave functions, $\{|\Phi(\beta_i)\rangle\}$.

3. Results

3.1. Energy curves

Figures 1 and 2 show the energy surfaces as functions of the quadrupole deformation parameter β for the positive- and negative-parity states, respectively, obtained by energy variation with a constraint on β after parity projection. The energies projected onto the $J^\pi = 0^+$, 3^-, and 4^- states are also shown.

In the positive-parity energy surface (Fig. 1), three excited local minima or shoulders exist around $\beta = 0.4$, 0.6, and 0.8 as well as the minimum at $\beta = 0.25$, which suggest the existence of three excited deformed bands in the positive-parity states. After AMP onto the $J^\pi = 0^+$ states, more deformed states gain more binding energy, and the β values of the local minima become larger. In the negative-parity energy surface (Fig. 2), three local minima exist around $\beta = 0.2$, 0.5, and 0.7. In the slightly deformed region, $\beta < 0.6$, the $J^\pi = 3^-$ components have the lowest energies after AMP. Highly deformed wave functions, $\beta > 0.6$, have few $J^\pi = 3^-$ components, and the $J^\pi = 4^-$ components have the lowest energies.

3.2. Level scheme and particle-hole configurations

Figure 3 shows the level scheme of the positive- and negative-parity states. Various rotational bands, called $K^\pi = 0^+_{\rm ND}$, $0^+_{\rm SD1}$, and $0^+_{\rm SD2}$ for positive parity and $K^\pi = 2^-_{\rm ND}$, $4^-_{\rm SD}$, and $3^-_{\rm SD}$ for negative parity, are obtained, as well as low-lying $0\hbar\omega$ and $1\hbar\omega$ states. The energies of the $0\hbar\omega$ and $1\hbar\omega$ states are consistent with experimental data.

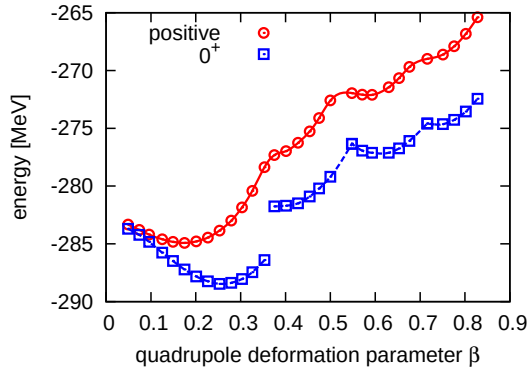

Figure 1. Energy surfaces as functions of quadrupole deformation parameter β for positive-parity states. Circles and squares show energies projected onto positive-parity and $J^\pi = 0^+$ states, respectively.

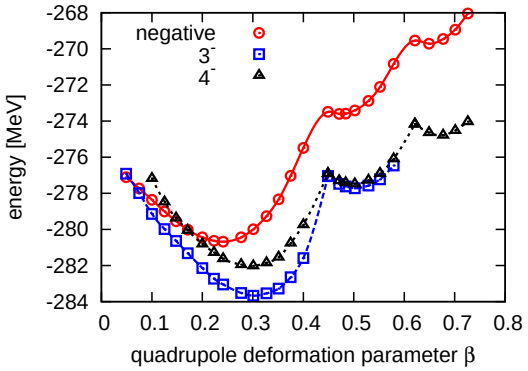

Figure 2. Energy surfaces as functions of quadrupole deformation parameter β for negative-parity states. Circles, squares, and triangles show energies projected onto positive-parity, $J^\pi = 3^-$, and $J^\pi = 4^-$ states, respectively.

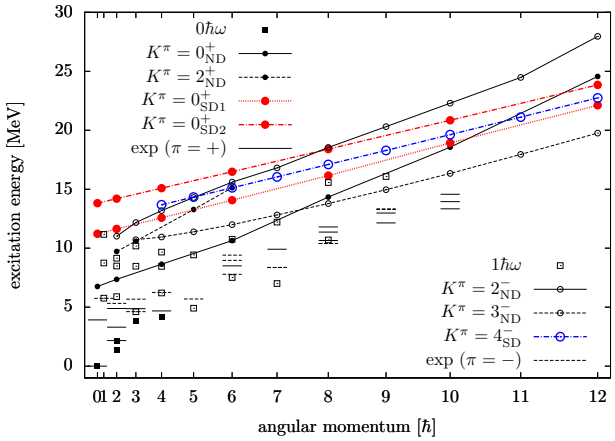

Figure 3. Excitation energies as functions of $J(J+1)$, where J is the total angular momentum. States with closed and open squares have dominant $0\hbar\omega$ and $1\hbar\omega$ configurations, respectively. Solid, dashed, dotted, and dot-dashed lines with closed circles show members of $K^\pi = 0^+_{\rm ND}$, $2^+_{\rm ND}$, $0^+_{\rm SD1}$, and $0^+_{\rm SD2}$ bands, respectively. Solid, dashed, and dot-dashed lines with open circles show members of $2^-_{\rm ND}$, $3^-_{\rm ND}$, and $4^-_{\rm SD}$ bands, respectively. Solid and dashed lines with no symbols show experimental values.

The members of the $K^\pi = 0^+_{\rm SD1}$, $0^+_{\rm SD2}$, and $4^-_{\rm SD}$ bands have mp-mh configurations for both the proton and neutron components; $(n_\pi, n_\nu) = (2,2)$, (2, 4), and (2, 3) for the $K^\pi = 0^+_{\rm SD1}$, $0^+_{\rm SD2}$, and $4^-_{\rm SD}$ bands, respectively, where n_π and n_ν are the numbers of protons and neutrons, respectively, excited from the *sd*-shell to the *pf*-shell. The values of the quadrupole deformation parameter β of dominant components of the SD bands are greater than 0.6. Their energies are within a few MeV, although the particle-hole configurations of the neutron components differ; they are $n_\nu = 2$, 3, and 4 for the $K^\pi = 0^+_{\rm SD1}$, $4^-_{\rm SD}$, and $0^+_{\rm SD2}$ bands, respectively. This shows the coexistence of two positive- and one negative-parity SD bands. The energy of the $K^\pi = 4^-_{\rm SD}$

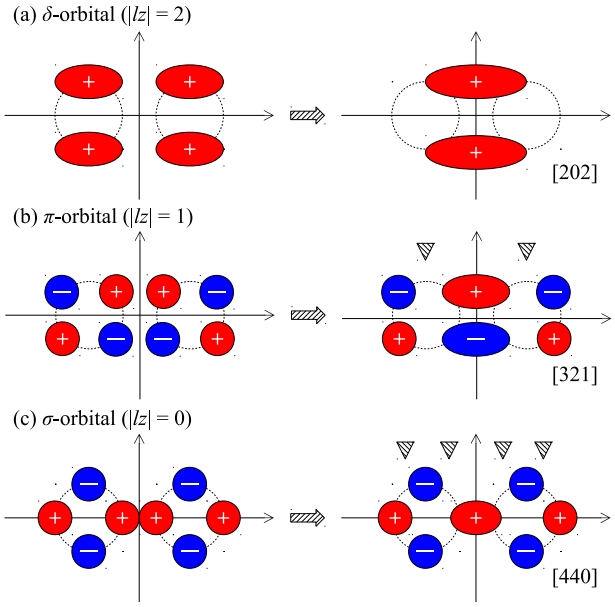

Figure 4. Schematic pictures of molecular orbitals generated from $0d$ orbits around two ^{16}O cores for (a) δ, (b) π, and (c) σ orbitals. Left and right columns show phases of $0d$ orbits around two ^{16}O cores and molecular orbitals, respectively. Dotted circles show two ^{16}O cores located on the z axis. Inverse triangles show locations of nodes in molecular orbitals in the z direction. Numbers in brackets show Nilsson quanta (see text).

band is intermediate between those of the $K^\pi = 0^+_{\rm SD1}$ and $0^+_{\rm SD2}$ bands.

The two highest single-particle orbits have $[202]^2$, $[321]^2$, and $[202]^1[321]^1$ configurations for the $K^\pi = 0^+_{\rm SD1}$, $0^+_{\rm SD2}$, and $4^-_{\rm SD}$ bands, respectively, in the Nilsson picture.

4. Discussions

4.1. Similarity of molecular orbitals around ^{16}O + ^{16}O cores and Nilsson orbits

Before discussing the structures of the SD states in ^{34}S, the quanta of molecular orbitals around the ^{16}O + ^{16}O cores are discussed in the Nilsson picture.

The lowest orbit around an ^{16}O core is a $0d_{5/2}$ orbit. By linear combination of $0d_{5/2}$ orbits around two ^{16}O cores, molecular orbitals around the two ^{16}O cores are formed. Figure 4 shows schematic illustrations of the formation of molecular orbitals around two spherical ^{16}O cores. Here, the two ^{16}O cores are located on the z axis (horizontal axis), and a cylindrical coordinate system is used in this section because of axial symmetry around the z axis.

The $0d_{5/2}$ orbits around the ^{16}O cores form δ, π, and σ orbitals, which are formed from two $(l, |l_z|) = (2, 2)$, $(2, 1)$, and $(2, 0)$ orbits, respectively, around the left and right ^{16}O cores. For the δ orbital, the $(l, |l_z|) = (2, 2)$ orbits have no node in the z direction, as shown in the left column of Fig. 4(a). Therefore, the δ orbital also has no node in the z direction, as shown in the right column of Fig. 4(a). Similarly, the numbers of nodes of the π and σ orbitals are two and four in the direction of the z axis, as shown in Figs. 4(b) and (c), respectively. In the radial direction, they have no node because a $0d$ orbit has no node in the radial direction. This shows that the quanta of the δ, π, and σ orbitals are [202], [321], and [440], respectively, in the Nilsson picture. When a system has a two-^{16}O core structure, the [202], [321], and [440] orbits correspond to the δ, π, and σorbitals, respectively. The parities of the δ, π, and σ orbitals are positive, negative, and positive, respectively.

4.2. Configurations of valence neutrons in the SD bands

The GCM calculation yielded three SD bands, called the $K^\pi = 0^+_{\rm SD1}$, $0^+_{\rm SD2}$, and $4^-_{\rm SD}$ bands, the structures of which are interpreted as ^{16}O + ^{16}O + two valence neutrons that have δ^2, π^2, and $\delta^1\pi^1$ configurations, respectively, in a cluster picture.

Their proton components have $2\hbar\omega$ excited configurations and neck structures, and the neutrons, except for the two highest-energy orbits, have the same configuration. This configuration is the same as that of the SD band in ^{32}S, which contains a large amount of ^{16}O + ^{16}O cluster structure components[3]. Therefore, the three SD bands have structures of ^{16}O + ^{16}O + valence neutrons in a cluster picture.

The configurations of the valence neutrons of the $K^\pi = 0^+_{\rm SD1}$, $0^+_{\rm SD2}$, and $4^-_{\rm SD}$ bands are $[202]^2$, $[321]^2$, and $[202]^1[321]^1$, respectively. As shown in the previous section, the [202] and [321] orbits correspond to the δ and π molecular orbitals, respectively, around the two ^{16}O cores. Therefore, the configurations of the valence neutrons of the $K^\pi = 0^+_{\rm SD1}$, $0^+_{\rm SD2}$, and $4^-_{\rm SD}$ bands are interpreted as δ^2, π^2, and $\delta^1\pi^1$, respectively.

5. Conclusions

The structure of the SD states in ^{34}S were investigated using the AMD and GCM. By superposing the AMD wave functions calculated via energy variation with a constraint on the quadrupole deformation parameter β, the coexistence of two positive- and one negative-parity SD bands is predicted. The SD states have mp-mh configurations, and they are interpreted as a structure consisting of ^{16}O + ^{16}O + valence neutrons in molecular orbitals around ^{16}O + ^{16}O cores in a cluster picture. Highly efficient γ spectroscopy experiments on high-spin states may reveal the structures of those deformed states.

Acknowledgments

This work was supported by JSPS KAKENHI Grant Number 25800124. The numerical calculations for this work were conducted under the Interdisciplinary Computational Science Program of the Center for Computational Sciences, University of Tsukuba.

References

[1] Inakura T, Mizutori S, Yamagami M and Matsuyanagi K 2003 *Nucl. Phys. A* **728** 52
[2] Ohkubo S and Yamashita K 2002 *Phys. Rev. C* **66** 021301
[3] Kimura M and Horiuchi H 2004 *Phys. Rev. C* **69** 051304
[4] Seya M, Kohno M and Nagata S 1981 *Prog. Theor. Phys.* **65** 204
[5] Kanada-En'yo Y, Horiuchi H and Doté A 1999 *Phys. Rev. C* **60** 064304
[6] Itagaki N and Okabe S 2000 *Phys. Rev. C* **61** 044306
[7] Ito M, Kato K and Ikeda K 2004 *Phys. Lett. B* **588** 43
[8] Ito M 2006 *Phys. Lett. B* **636** 293
[9] Ito M, Itagaki N, Sakurai H and Ikeda K 2008 *Phys. Rev. Lett.* **100** 182502
[10] Ito M, Itagaki N and Ikeda K 2012 *Phys. Rev. C* **85** 014302
[11] Kanada-En'yo Y, Kimura M and Ono A 2012 *Prog. Theor. Exp. Phys.* **2012** 01A202
[12] Mason P, Mărginean N, Lenzi S M, Ionescu-Bujor M, Della Vedova F, Napoli D R, Otsuka T, Utsuno Y, Nowacki F, Axiotis M, Bazzacco D, Bizzeti P G, Bizzeti-Sona A, Brandolini F, Cardona M, de Angelis G, Farnea E, Gadea A, Hojman D, Iordachescu A, Kalfas C, Kröll T, Lunardi S, Martínez T, Petrache C M, Quintana B, Ribas R V, Rossi Alvarez C, Ur C A, Vlastou R and Zilio S 2005 *Phys. Rev. C* **71** 014316